

## Numerical Study of Green Water Loads on a Fixed Structure by MPS Method

Mengmeng Wu<sup>1</sup>, Jifei Wang<sup>2</sup>, Weiwen Zhao<sup>1</sup>, Decheng Wan<sup>1\*</sup>

<sup>1</sup> Computational Marine Hydrodynamic Lab (CMHL), School of Naval Architecture, Ocean and Civil Engineering, Shanghai Jiao Tong University, Shanghai, China

<sup>2</sup> Shanghai Aerospace System Engineering Institute, Shanghai, China

\*Corresponding Author

### ABSTRACT

In rough sea conditions, large mass of water will exceed the freeboard and cause violent slamming on the deck which is known as green water. Due to the strong destructiveness, many scholars have devoted to the study of green water. Considering the complexity, different simplified methods were used to study the mechanism and loads of green water. Among them, the wet dam-break method is an effective and convenient way to generate strong wave impacts. This paper investigated green water loads and patterns on a fixed structure using meshless particle solver MLParticle-SJTU based on Moving Particle Semi-Implicit (MPS) method. The rapid flow-structure interaction is generated by wet dam-break method. The experimental study (Hernández-Fontes et al., 2020) investigated vertical loads of green water and the numerical work (Areu-Rangel et al., 2021) continued to study horizontal loads. In this paper, the study is extended by analyzing the effects of different gate release velocities on the generated wave patterns and green water loads. The results obtained in this paper are in good agreement with the existing results. And the influence of different gate release speeds on the green water simulation is analyzed.

**KEY WORDS:** Green water; Moving Particle Semi-Implicit (MPS); wave loads; wet dam-break method; gate release.

### INTRODUCTION

Marine structures are vulnerable to wave intrusion. In severe sea conditions, these incoming waves are likely to exceed the freeboard, board the deck and spread on the deck. This phenomenon is called green water or water shipping (Greco et al., 2004). Green water in harsh sea conditions will cause adverse effects, such as damage to superstructure and hull structure, accidental overload of ships, injury to humans, equipment damage, etc. For ships and other marine structures, it is of great practical significance to study the physical mechanism of the wave on the deck, predict the wave on the deck and assess of the impact on the safety and performance of ships and offshore platforms.

The phenomenon of green water has been studied by experimental

(Fonseca et al., 2005), theoretical (Zhang et al., 1996) and numerical methods. The current research mainly focuses on the identification of types of green water events (Greco et al. 2007), the evolution process of the water on the deck (Le Touzé et al., 2010), the wave loads (Nielsen et al., 2004) and so on. With the development of computer technology, Computational Fluid Dynamics (CFD) methods based on the meshless method and mesh-based method (Rosetti et al., 2019; Silva et al., 2017) have been used to study the green water phenomena. The mesh method needs to introduce special free surface processing methods when dealing with problems such as wave surface rolling, crushing and splashing. Compared with the mesh-based method, the particle-based methods do not require additional interface capture or reconstruction algorithms, and can track free surfaces with any large deformation. It has natural advantages in simulating large deformation of free surface (Luo et al., 2021), and scholars have done a lot of research work, for instance, dam-break flow (Tang et al., 2016; Chen and Wan, 2019), water entry problems (Tang et al., 2016), the liquid sloshing problems (Zhang et al., 2014), wave-ship interaction (Shibata et al., 2012), multiphase flow (Wen et al., 2021), fluid-structure interaction (Zhang et al., 2019; Khayyer et al., 2017) and so on.

Many scholars used particle methods to study the phenomenon of green water. In order to generate incident waves of severe sea conditions, regular wave, solitary wave and other methods are used in investigating the problem of green water using particle method. Shibata et al. (2007) simulated the water shipping phenomenon on the bow deck of a three-dimensional fixed ship under the action of solitary waves, using the MPS method to predict the impact pressure on the deck. The wave pattern, wave height and impact pressure on the deck were compared with the experiment, and good consistency is obtained. Kawamura et al. (2016) applied the Smoothed Particle Hydrodynamics (SPH) method to predict the motion of fishing vessel under green water conditions produced by steep regular wave and this SPH simulation presented the shipping water events and wave reflection well. Based on the MPS method, Zhang et al. (2016) studied the green water phenomenon of solitary waves impacting a plate structure, analyzed the trend of the impact loads on the plate and the wave evolution process under the interaction between solitary waves and structures.

Green water events are complex phenomena that occur rapidly. To investigate the features and loads generated by isolated green water events, systematic alternative wet dam-break method has been used to generate the incident wave in recent studies. The wet dam-break method is similar to the dam-break phenomenon. The wet dam-break can be regarded as adding a certain height of water downstream of the dam-break. Khayyer and Gotoh (2011) simulated the wave generated by wet dam-break method using standard and improved versions of three particle methods, namely the MPS, the Incompressible Smoothed Particle Hydrodynamics (ISPH) and the Weakly Compressible Smoothed Particle Hydrodynamics (WCSPH) method, and compared results with experiments. The work highlighted the potential capabilities of particle methods in reproducing detailed features of wet dam-break. The dam break wave flowing over dry and wet beds were investigated experimentally and numerically by Garoosi et al. (2022). It was found that, although both MPS and Volume-Of-Fluid (VOF) models were capable of capturing morphological changes of dam break flows, the MPS in general outperformed the VOF in handling nonlinear multiphase phenomena involving wave breaking and splashing. This verified the accuracy of MPS method in wet dam-break simulation.

The experimental study by Hernández-Fontes et al. (2020) investigated vertical loads of a fixed structure in the case of water shipping and the numerical work by Areu-Rangel et al. (2021) further investigated horizontal loads. In these studies, the green water events were generated by the wet dam-break method. Wet dam-break method is very friendly to both experiments and numerical simulations in analyzing different green water events because it is simple and can produce systematic, repeatable and short-duration green water events. In order to realize the condition of wet dam-break method in experiment, a gate was used to control the water at the beginning of the experiment. It can be seen that the incident waves of experiment of Hernández-Fontes et al. (2020) with gate and the numerical simulation of Areu-Rangel et al. (2021) without gate produced different incident wave patterns. This shows that the gate had a certain influence on the wave formation and the green water events generated. This paper would analyze the differences among the green water events generated by the wet dam-break method caused by different gate release speeds.

von Häfen et al. (2019) investigated the effect of different gate speeds on the waveform formed by dam-break method based on experiments and SPH simulations. The motion of the gate resulted in difference associated with the propagation of the wave. The slower the gate opening, the greater the difference. The difference was particularly pronounced in the near-field and decreased with increasing distance from the gate. Ye and Zhao (2017) used a two-liquid VOF-based model to investigate the influence of gate removal velocity on the early stages of wet dam-break flow. The gate release speed affected the evolution of the free surface and water-water interface profiles. With an increase in gate velocity, the formation and evolution of jet flow and dam break wave would become earlier. Obviously, existing research is not enough.

In order to better analyze the effects of the gate release speeds in wave patterns and loads of green water events generated in the model used by Areu-Rangel et al. (2021) and Hernández-Fontes et al. (2020), this paper used meshless particle solver MLPparticle-SJTU based on MPS method to simulate the water shipping events under different gate release speeds.

## NUMERICAL METHOD

The MPS method is a meshless particle method and discretizes the fluid and solid part in a set of particles endowed with physical characteristics such as mass, velocity and acceleration and so on (Koshizuka and Oka, 1996). These particles interact through kernel function. As the distance

between particles becomes smaller, the interaction between them becomes greater. The fluid is controlled by the governing equation based on Lagrangian method.

## Governing equation

The governing equations include the continuity equation and the momentum equation. The governing equation for viscous incompressible flow can be written as:

$$\frac{1}{\rho} \frac{D\rho}{Dt} = -\nabla \cdot \mathbf{V} = 0 \quad (1)$$

$$\frac{D\mathbf{V}}{Dt} = -\frac{1}{\rho} \nabla P + \nu \nabla^2 \mathbf{V} + \mathbf{g} \quad (2)$$

where:  $\rho$  is the fluid density,  $\mathbf{V}$  is the velocity vector,  $P$  presents the pressure,  $\nu$  is the kinematic viscosity,  $\mathbf{g}$  is gravitational acceleration vector,  $t$  indicates the time. In this paper, the fluid density  $\rho$  is  $10^3 \text{ kg/m}^3$  and the kinematic viscosity  $\nu$  is  $1.01 \times 10^{-6} \text{ m}^2/\text{s}$ .

## Kernel function

In the MPS method, the interaction between particles is realized by the kernel function (Koshizuka and Oka, 1996; Ataie-Ashtiani and Farhadi, 2006). The kernel function of the improved MPS method (Zhang et al., 2014) is shown as follows:

$$W(r) = \begin{cases} \frac{r_e}{0.85r + 0.15r_e} - 1 & 0 \leq r < r_e \\ 0 & r_e \leq r \end{cases} \quad (3)$$

where:  $r = |\mathbf{r}_j - \mathbf{r}_i|$  represents the spacing between particle  $i$  and  $j$  and  $r_e$  is the influence radius. Generally, the influence radius for particle number density and the gradient model is  $r_e = 2.1l_0$  and it is  $r_e = 4.1l_0$  for the Laplacian model in this paper, where  $l_0$  is the initial particle space.

## Density of the particle number

The particle number density is the sum of all particle kernel functions within the radius of influence. It is defined as:

$$\langle n \rangle_i = \sum_{j \neq i} W(|\mathbf{r}_j - \mathbf{r}_i|) \quad (4)$$

For incompressible fluid, the particle number density is constant.

## Gradient model

The gradient model is used to discretize the pressure gradient in the governing equation. The expression is:

$$\langle \nabla P \rangle_i = \frac{D}{n^0} \sum_{j \neq i} \frac{P_j + P_i}{|\mathbf{r}_j - \mathbf{r}_i|^2} (\mathbf{r}_j - \mathbf{r}_i) W(|\mathbf{r}_j - \mathbf{r}_i|) \quad (5)$$

where  $D$  represents the dimension and  $n^0$  represents the initial particle number density.

## Divergence model

Similar to the gradient model, the divergence model is used to discretize the velocity divergence in the governing equation. The expression is:

$$\langle \nabla \cdot \mathbf{V} \rangle_i = \frac{D}{n^0} \sum_{j \neq i} \frac{(\mathbf{V}_j - \mathbf{V}_i) \cdot (\mathbf{r}_j - \mathbf{r}_i)}{|\mathbf{r}_j - \mathbf{r}_i|^2} W(|\mathbf{r}_j - \mathbf{r}_i|) \quad (6)$$

## Laplacian model

Laplacian model is used to discretize the second derivative in the governing equation, which can be expressed as:

$$\langle \nabla^2 \phi \rangle_i = \frac{2D}{n^0 \lambda} \sum_{j \neq i} (\phi_j - \phi_i) W(|\mathbf{r}_j - \mathbf{r}_i|) \quad (7)$$

where  $\phi$  is an arbitrary scalar function,  $\lambda$  represents the correction of the error introduced by the kernel function, and it can be written as:

$$\lambda = \frac{\sum_{j \neq i} W(|\mathbf{r}_j - \mathbf{r}_i|) |\mathbf{r}_j - \mathbf{r}_i|^2}{\sum_{j \neq i} W(|\mathbf{r}_j - \mathbf{r}_i|)} \quad (8)$$

### Pressure Poisson equation

In the MPS method, the Poisson equation is used to solve the particle pressure (Khayyer and Gotoh, 2011). The incompressibility of fluid is determined by divergence-free condition and constant particle number density condition. The Poisson equation adopted in this paper is as follows:

$$\langle \nabla^2 P^{k+1} \rangle_i = (1-\gamma) \frac{\rho}{\Delta t} \nabla \cdot \mathbf{V}_i^* - \gamma \frac{\rho}{\Delta t^2} \frac{\langle n^k \rangle_i - n^0}{n^0} \quad (9)$$

Superscripts  $k$  and  $k+1$  represent  $k$  and  $k+1$  time steps.  $\gamma$  is a variable parameter, representing the proportion of particle number density in the source term of Poisson equation. In the numerical simulation in this paper,  $\gamma$  takes 0.01 (Tanaka and Masunaga, 2010).  $\mathbf{V}_i^*$  is the temporary velocity vector and the superscript  $*$  stands for the temporary value, which will be introduced below.

### Time integration

The procedure of MPS method is divided into two substeps for every time step. First, all terms except the pressure term in the momentum conservation equation are evaluated explicitly, and the temporal velocity vectors and position vectors of particles are computed as

$$\mathbf{V}_i^* = \mathbf{V}_i^k + \Delta t (\mathbf{v} \nabla^2 \mathbf{V}_i^k + \mathbf{g}) \quad (10)$$

$$\mathbf{r}_i^* = \Delta t \cdot \mathbf{V}_i^* + \mathbf{r}_i^k \quad (11)$$

Second, the pressure term is solved implicitly according to the Pressure Poisson equation by the bi-conjugate gradients stabilized (Bi-CGSTAB) method. Then, the velocity vectors and position vectors of particles are modified as

$$\mathbf{V}_i^{k+1} = \mathbf{V}_i^* - \frac{\Delta t}{\rho} \nabla P^{k+1} \quad (12)$$

$$\mathbf{r}_i^{k+1} = \Delta t \cdot \mathbf{V}_i^{k+1} + \mathbf{r}_i^k \quad (13)$$

### Detection of free surface particles

Once a fluid particle is judged to be located on the free surface, the pressure of it will be forced to be zero and this will be used as the boundary condition for solving the pressure Poisson equation. In consequence, it is important to determine whether a particle is located on free surface. The number density of particles can be used to determine whether a particle is on a free surface in MPS method. When  $\langle n \rangle_i < 0.8n^0$ , the particle is considered to be on a free surface. When  $\langle n \rangle_i > 0.97n^0$ , the particles are thought to be inside the fluid. For particles with particle number density between 0.8 and 0.97, it's difficult to distinguish whether the particle is free surface particle or the internal particle. In this paper, the vector function  $\mathbf{F}$  presented by Zhang et al (2014) is introduced, as follows:

$$\langle \mathbf{F} \rangle_i = \frac{D}{n^0} \sum_{j \neq i} \frac{(\mathbf{r}_i - \mathbf{r}_j)}{|\mathbf{r}_i - \mathbf{r}_j|} W(|\mathbf{r}_i - \mathbf{r}_j|) \quad (14)$$

where  $\mathbf{F}$  is a vector which represents the asymmetry distribution of neighboring particles. When  $\langle |\mathbf{F}| \rangle_i > 0.9|\mathbf{F}|^0$ , the particle is considered to be on the free surface.  $|\mathbf{F}|^0$  stands for  $|\mathbf{F}|$  at the initial time of the free surface particle.

### Boundary condition

In this paper, the solid boundary is represented by one layer of wall particles and two layers of ghost particles. The calculation of pressure on wall particles is the same as that of fluid particles, solving by PPE. Whereas the pressures of ghost particles are obtained by interpolation. The advantage of this arrangement is that it can ensure a smooth and accurate pressure field around the solid surface and prevent fluid particles from penetrating into the impermeable boundary. The velocity and displacement of the wall particles and ghost particles were specified in the MPS simulation of this paper.

## NUMERICAL SIMULATIONS

### Validation of MPS method

Firstly, the effectiveness of the MPS method and the solver MLParticle-SJTU was verified by the above mentioned SPH simulation (Aren-Rangel et al., 2021). SPH simulation used the wet dam-break method to generate the incident wave, and a fixed rectangular structure was placed on the right side of the tank. The right wall of the tank can be regarded as the side wall of the superstructure on the fixed structure.

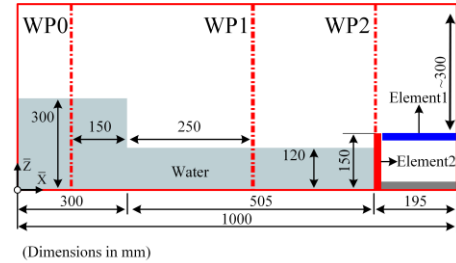


Fig. 1 The sketch of the water shipping model studied by Aren-Rangel (2021), indicating the positions of the three wave probes and two structural elements for the investigation of the hydrodynamic loads.

The simulation model of Aren-Rangel et al. is shown in Fig. 1. Three wave probes WP0, WP1 and WP2 have been arranged. The upper part of the right side two-dimensional fixed structure is a force measuring element with a length of 0.18 m and a 0.15 m high force measuring element is arranged on the left side of the structure. These settings were to measure water elevations of the incident wave (WP0 and WP1, Fig. 1), freeboard exceedance (WP2, Fig. 1), vertical loads on the deck (Element 1, Fig. 1) and the horizontal loads of left side of structure. The remaining specific dimensions are also shown in Fig. 1.

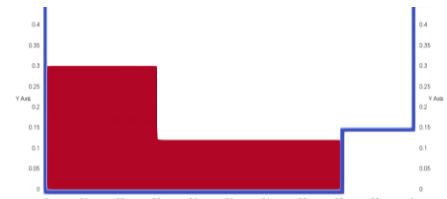


Fig. 2 The sketch of the model used in validation of MPS simulation.

In order to save computing resources, the model showed in Fig. 2 was used in MPS simulation, which can achieve the same simulation goals as Areu-Rangel et al. Corresponding to the simulation of SPH, the start time of MPS simulation in this paper was also set to 0.5 s. The simulation time interval was 0.0002 s, and the initial particle spacing was 0.001 m in this paper while the time-step algorithm used was the Verlet and the initial particle spacing was 0.0005 m in SPH simulation.

Fig. 3 shows the velocity field comparison diagram of SPH simulation and the simulation of the MLParticle-SJTU solver used in this paper. It can be seen that the wave patterns and velocity fields of these two simulations were very similar. After the incident wave reached the left side of the structure, it broke, then the incident wave attacked the upper deck of the structure and climbed up along the right side of the tank wall, then fell back and flowed down from the deck. In this process, a cavity appeared near the left edge of the deck and then disappeared.

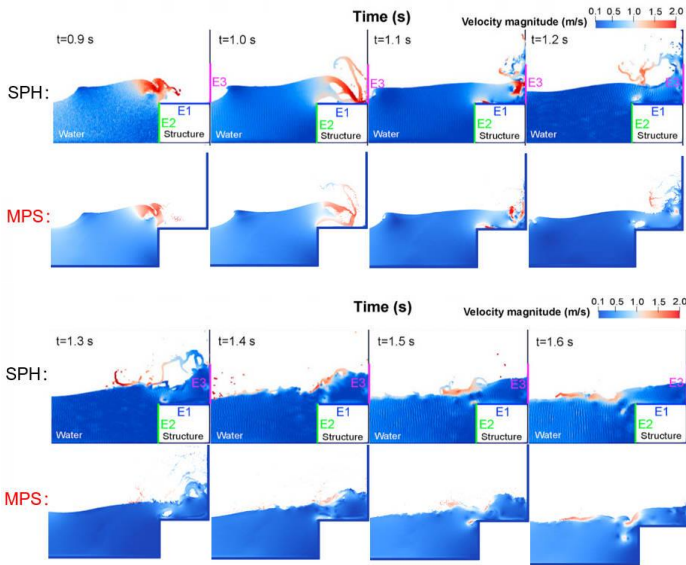
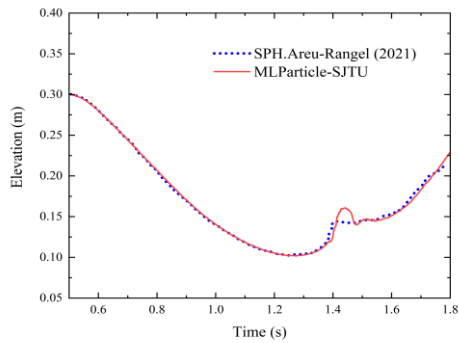
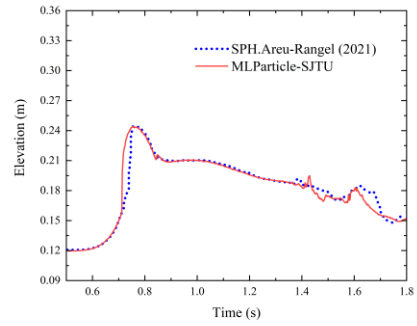


Fig. 3 Snapshots of the velocity fields of some relevant stages observed during the simulations using the SPH method (Areu-Rangel et al., 2021) and the MPS method.

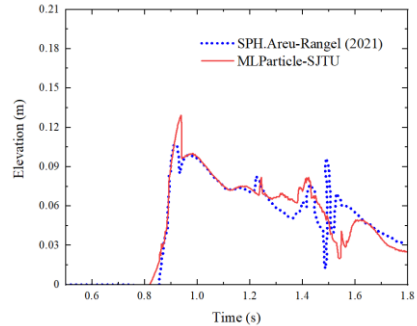
It can be seen from the water elevations measured at WP0, WP1 and WP2 in Fig.4 that the elevations of SPH and MPS simulation were roughly the same, which proved that the wave patterns of MPS simulation and SPH simulation in the left side of the tank were basically the same.



a) WP0

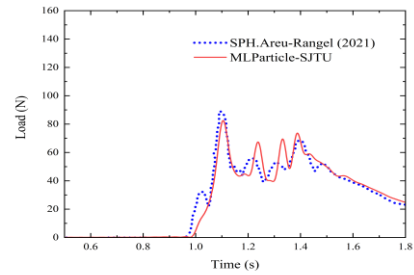


(b) WP1

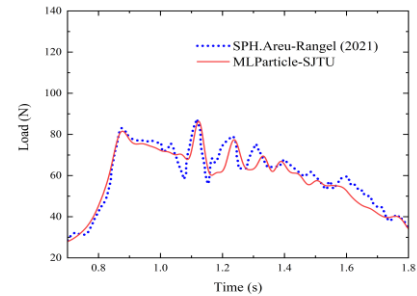


(c) WP2

Fig. 4 Validation of the numerical approach: comparison of the wave elevations between the SPH results and MPS results. (a) Water elevations at WP0. (b) Water elevations at WP1. (c) Water elevations at WP2.



(a) Element1



(b) Element2

Fig. 5 Validation of the numerical approach: comparison of the loads of elements between the SPH results and MPS results. (a) Vertical loads of element 1. (b) Horizontal loads of element 2.

Fig. 5 shows the loads on Element1 and Element2, and the results of SPH and MPS were highly consistent in terms of trends and values. In summary, the numerical simulation results using the MPS method shown in this paper had a high similarity with the results of Areu-Rangel et al., which verified the accuracy of the numerical simulation method used in this paper. This simulation model can be used for the next numerical simulations.

### Effect of the gate release velocity in wave pattern and loads

In order to study the influence of the gate release on the wave formation and the green water events generated, four different gate release speeds were used to generate incident waves, which were 1m/s, 1.6m/s, 2m/s, and 5m/s, respectively. The gate moved vertically in a uniform linear motion without acceleration. The thickness of the gate is 0.01 m, which is the same as the experimental setting of Hernández-Fontes et al. (2020).

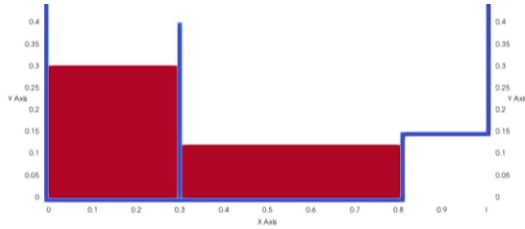


Fig. 6 The sketch of the model used in MPS simulation.

The numerical simulation model and settings used are shown in Fig. 6, which is consistent with the model of the above verification procedure, except for a gate with a width of 0.01 m. The settings of three wave probes and two elements are the same with information shown in Fig. 1.

Hernández-Fontes et al. (2020) showed the results of the wet dam-break experiment of the same model as this paper, but did not provide information about the gate release speed. The results of this experiment were also compared with the results of MPS simulation.

Figs. 7~12 show representative snapshots of the experiments of Hernández-Fontes et al. (2020) and MPS simulations at different gate release speeds, it can be seen that when the gate release speed was 1.6 m/s, the wave patterns of numerical simulation were almost consistent with the experimental data. When the gate speed was less than 2 m/s, the incident wave at 0.97s was relatively complete. Broken bores can be observed in the cases of higher speeds.

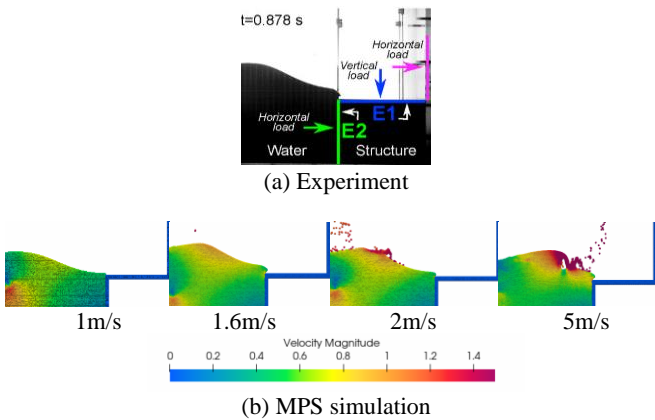
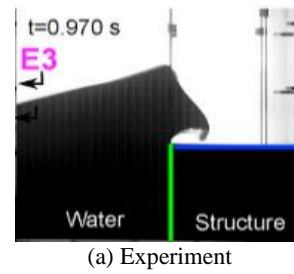
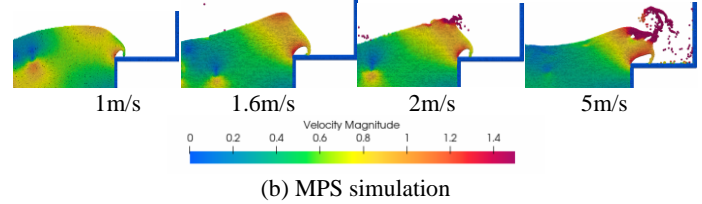


Fig. 7 Snapshots found in the experiment of Hernández-Fontes et al. (2020) and MPS simulations with different gate speed at 0.878s.

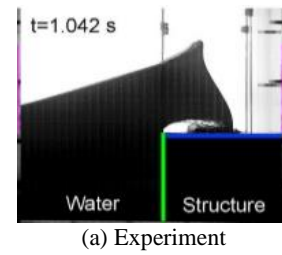


(a) Experiment

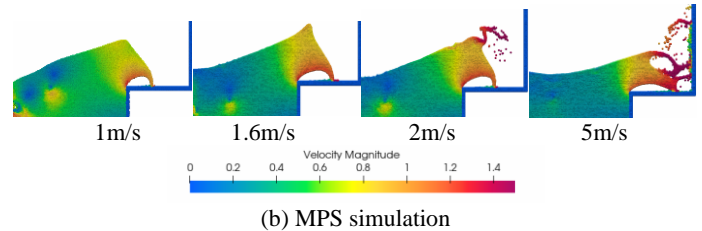


(b) MPS simulation

Fig. 8 Snapshots found in the experiment of Hernández-Fontes et al. (2020) and MPS simulations with different gate speed at 0.970s.

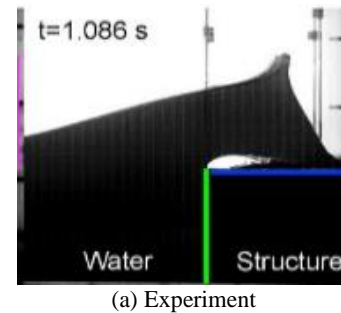


(a) Experiment

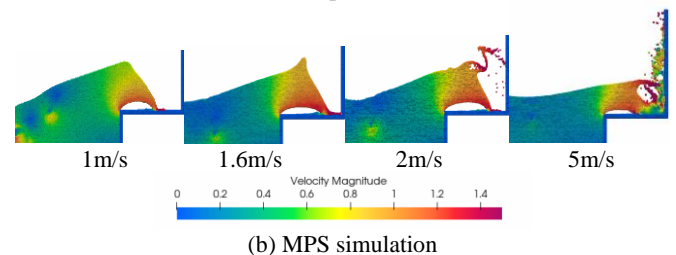


(b) MPS simulation

Fig. 9 Snapshots found in the experiment of Hernández-Fontes et al. (2020) and MPS simulations with different gate speed at 1.042s.



(a) Experiment



(b) MPS simulation

Fig. 10 Snapshots found in the experiment of Hernández-Fontes et al. (2020) and MPS simulations with different gate speed at 1.086s.

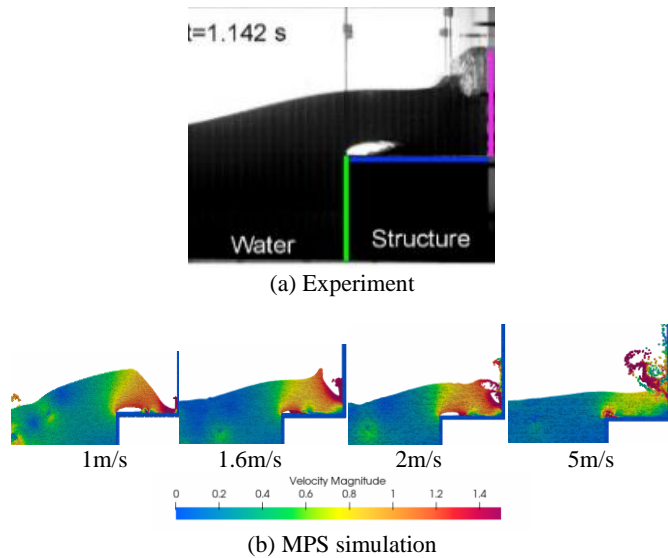


Fig. 11 Snapshots found in the experiment of Hernández-Fontes et al. (2020) and MPS simulations with different gate speed at 1.142s.

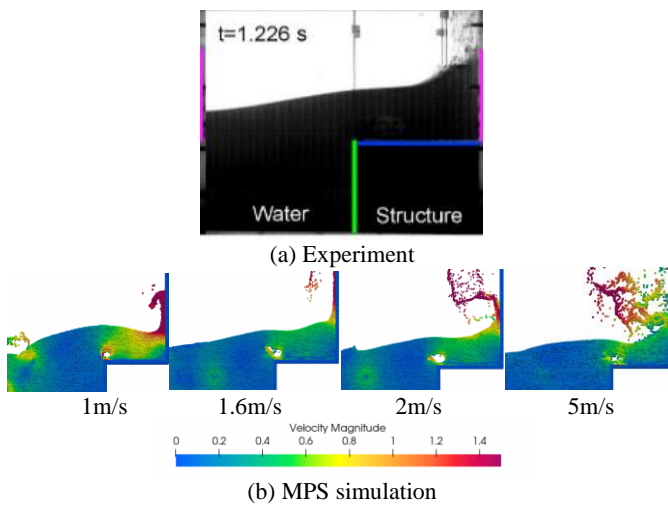


Fig. 12 Snapshots found in the experiment of Hernández-Fontes et al. (2020) and MPS simulations with different gate speed at 1.226s.

Figs. 13~14 show that different gate release speeds produced different incident waves of green water events. In the cases of small gate speeds, the water on the left of the gate flowed from the gap under the gate into the lower part of the water on the right. The water on the right-hand side was then jacked up and propagated towards the fixed structure. Next, the water on the left of the structure rose and formed the incident wave of the green water events. With high gate release speeds, the interaction time between the gate and the water was short and the water did not deform much when the gate left the water, as shown in Figure 13. With the gate speed of 5m/s, the flow field was close to the flow field generated by the ideal wet dam-break method without a gate. After the gate left the water on the left side of the gate, the two bodies of water of different heights squeezed each other to form a wave at the middle junction. This wave propagated to the right. When it reached the structure, it encountered the water coming up from the left side of the structure as shown in Fig.7~8, resulting in the broken incident wave of green water events. In other words, the way in which the incident wave of the green water event was generated was different for different gate release speeds. It can also be seen that in the case of low gate speed, the water body with

high kinetic energy was below the water surface, and in the case of high gate speed, the water body with high kinetic energy was on the free surface.

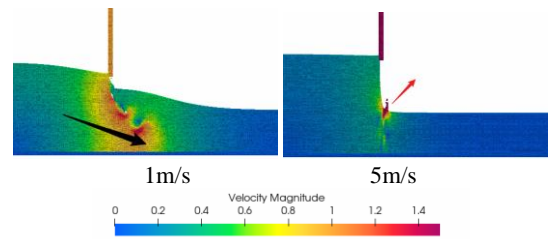


Fig. 13 Snapshots of the moments contact of gate and water ends.

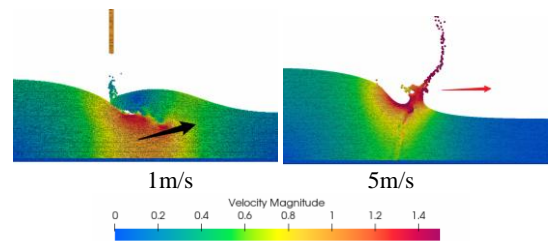
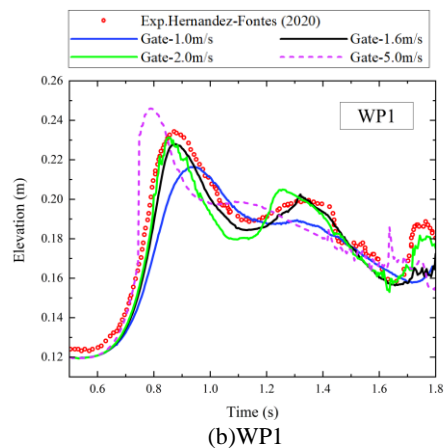
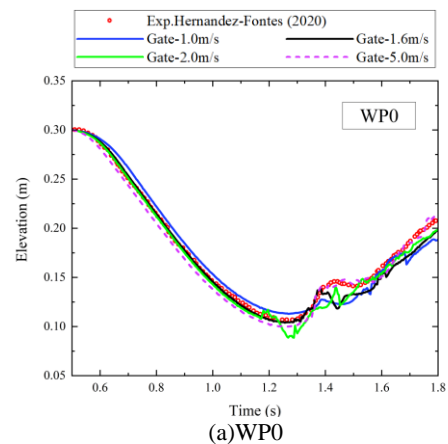


Fig. 14 Snapshots of the different incident waves generated by different gate speeds.



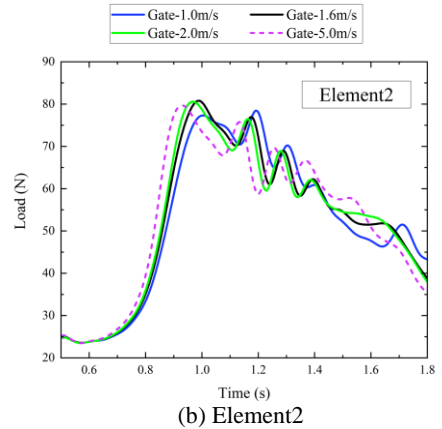
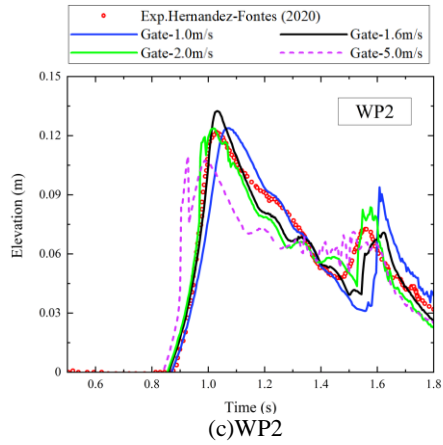


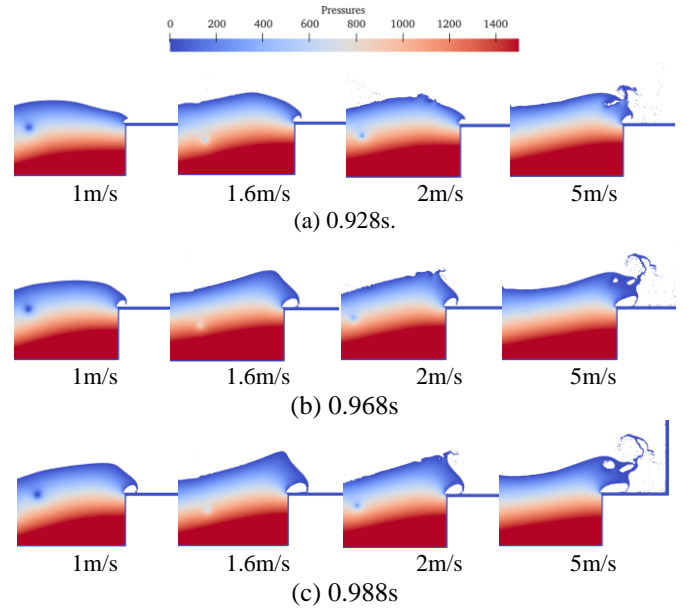
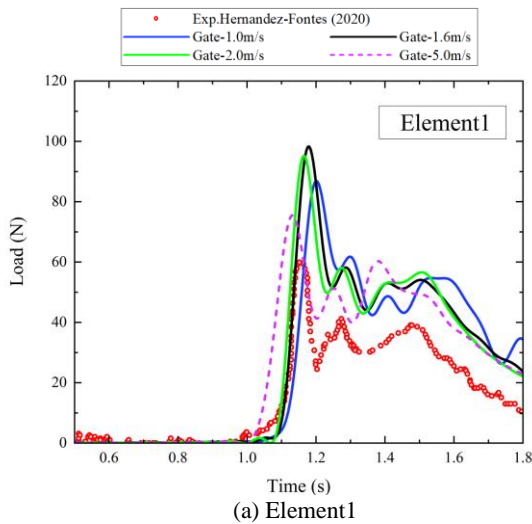
Fig. 15 Wave elevations at different gate release speeds and wave elevations of experiment (Hernández-Fontes et al., 2020). (a) Water elevations at WP0. (b) Water elevations at WP1. (c) Water elevations at WP2.

It can be seen from the elevation curves (Fig.15) at WP0 that the slower the gate speed, the slower the left water body dropped. This was due to the blocking effect of the gate on the left water body. From the elevation curves (Fig.15) at WP1, it can be seen that as the gate speed increased, the peak value of elevation at WP1 increased, and the peak value of the elevation arrived earlier. The gate release speeds were different, the way of generating incident waves was different, and the speeds of wave propagation were also different. Similarly, the higher the gate speed, the earlier the peak value of WP2 reached. In the case of large gate release speed, wave collision and breaking were more likely to occur at the WP2, resulting in a decrease in the peak value of wave height. When the gate release velocity was too low, the blocking effect of the gate was stronger and the interaction time between water and gate was longer, resulting in less kinetic energy of incident wave of green water event and the decrease in the peak value of the elevation at WP2. The influence of gate release velocity on the water elevation of WP0 was less than that on WP1 and WP2 downstream.

In addition, the experimental results of Hernández-Fontes et al. are compared with the MPS numerical simulation results in Fig. 15, which verifies the accuracy of wave patterns in the numerical simulation to some extent.

Fig. 16 Loads of elements at different gate release speeds and loads of elements of experiment (Hernández-Fontes et al., 2020). (a) Vertical loads of element 1. (b) Horizontal loads of element 2.

From the vertical load of Element1 (Fig. 16), it can be seen that the larger the gate release speed, the earlier the peak of load was reached, which was similar to the trend of the elevation curve of WP2. The maximum vertical loads occurred when the incident wave hit the upper deck in a large area. The peak value of vertical load of Element1 at the gate speed of 1.6m/s was the largest. The low gate speed would contribute to less kinetic energy of the incident wave in the green water event and less volume of water hitting deck, resulting in a reduction of the peak load value. If the gate speed was too high, waves would collide and break near the left wall of the structure, and some of the water would be hindered and flow back into the tank, reducing the water volume of the green water event and the peak value of load. The effect of gate release speed on peak value of horizontal load on Element2 was similar to that on the peak value of wave elevation at WP2. In addition to hydrostatic pressure, the kinetic energy and the velocity of the water on the left side of the structure also influenced the horizontal load of element 2. Therefore, the relationships of the peak loads of element 2 and the wave elevations at the WP2 measuring point were slightly different.



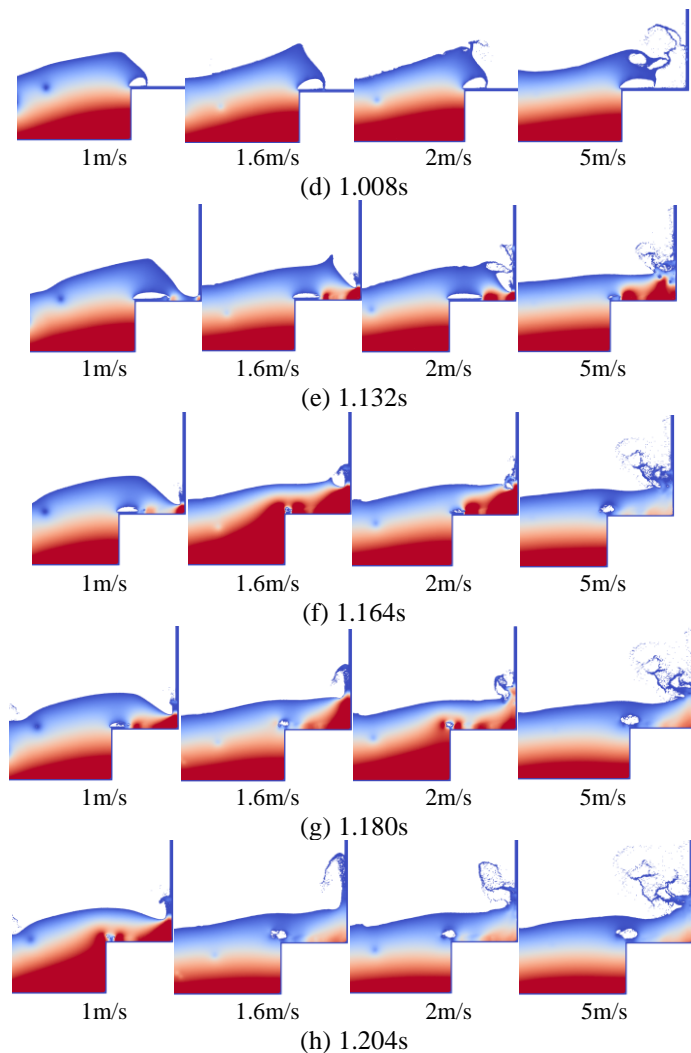


Fig. 17 Snapshots of pressure fields found in MPS simulations with different gate speed at different time.

Fig. 17 shows snapshots of the pressure fields at the moments of peak loads. Significant pressures occurred at the connection between the superstructure and the deck of the structure, which was detrimental to the structure.

In addition, the load on the structure in experiment of Hernández-Fontes was much lower than that in the MPS simulation when the gate speed is 1.6 m/s, which may be due to the cavity generated at the left edge of the structure deck. The numerical simulation in this paper did not consider the air phase, which would have a certain impact on the results. Nevertheless, the trend of the experimental load was very similar to the numerical simulation result of the gate speed of 1.6 m/s, which indicated that the analysis in this paper was still effective.

## CONCLUSIONS

In this paper, the solver MlParticle-SJTU based on MPS method was used to simulate and analyze the influence of different gate release speeds on the incident wave patterns generated by the wet dam-break method and the loads of the fixed structure under the given model parameters. Through the analysis of the results, some conclusions can be drawn. Firstly, the simulations with different gate release speeds

generated incident waves in different ways and the wave patterns were different. The greater the speed, the more likely the incident wave was broken before boarding the deck. Secondly, the greater the release speed of the gate, the earlier the wave loads of the structure reached the peak. Thirdly, the peak values of the wave loads reached the maximum at a certain release speed. As the release speed of the gate increased or decreased, the peak values of the wave loads decreased. The results of this paper can provide reference for subsequent experiments or numerical simulations based on the wet dam-break method.

## ACKNOWLEDGEMENTS

This work was supported by the National Natural Science Foundation of China (52131102), and the National Key Research and Development Program of China (2019YFB1704200), to which the authors are most grateful.

## REFERENCES

- Areu-Rangel, OS, Hernández-Fontes, JV, Silva, R, Esperanca, PTT, and Klapp, J (2021). "Green water loads using the wet dam-break method and SPH," *Ocean Engineering*, 219, 108392.
- Ataie-Ashtiani, B, and Farhadi, L (2006). "A stable moving-particle semi-implicit method for free surface flows," *Fluid Dynamics Research*, 38(4), 241-256.
- Chen, X, and Wan, D (2019). "GPU accelerated MPS method for large-scale 3-D violent free surface flows," *Ocean Engineering*, 171, 677-694.
- Fonseca, N, and Soares, CG (2005). "Experimental investigation of the shipping of water on the bow of a containership," *Journal of Offshore Mechanics and Arctic Engineering-Transactions of The Asme*, 127(4), 322-330.
- Garoozi, F, Mellado-Cusichua, AN, Shademani, M, and Shakibaenia, A (2022). "Experimental and numerical investigations of dam break flow over dry and wet beds," *International Journal of Mechanical Sciences*, 215, 106946.
- Greco, M, Colicchio, G, and Faltinsen, OM (2007). "Shipping of water on a two-dimensional structure. Part 2," *Journal of Fluid Mechanics*, 581, 371-399.
- Greco, M, Landrini, M, and Faltinsen, OM (2004). "Impact flows and loads on ship-deck structures," *Journal of Fluids and Structures*, 19(3), 251-275.
- Häfen von, H, Goseberg, N, Stolle, J, and Nistor, I (2019). "Gate-Opening Criteria for Generating Dam-Break Waves," *Journal of Hydraulic Engineering*, 145(3), 04019002.
- Hernández-Fontes, JV, Vitola, MA, Esperanca, PTT, Sphaier, SH, and Silva, R (2020). "Patterns and vertical loads in water shipping in systematic wet dam-break experiments," *Ocean Engineering*, 197, 106891.
- Kawamura, K, Hashimoto, H, Matsuda, A, and Terada, D (2016). "SPH simulation of ship behaviour in severe water-shipping situations," *Ocean Engineering*, 120, 220-229.
- Khayyer, A, and Gotoh, H (2010). "On particle-based simulation of a dam break over a wet bed," *Journal of Hydraulic Research*, 48(2), 238-

- Khayyer, A, and Gotoh, H (2011). "Enhancement of stability and accuracy of the moving particle semi-implicit method," *Journal of Computational Physics*, 230(8), 3093-3118.
- Khayyer, A, Gotoh, H, Falahaty, H, Shimizu, Y, and Nishijima, Y (2017). "Towards development of a reliable fully-Lagrangian MPS-based FSI solver for simulation of 2D hydroelastic slamming," *Ocean Systems Engineering*, 7(3), 299-318.
- Koshizuka, S, and Oka, Y (1996). "Moving-Particle Semi-Implicit Method for Fragmentation of Incompressible Fluid," *Nuclear Science and Engineering*, 123(3), 421-434.
- Le Touzé, D, Marsh, A, Oger, G, Guilcher, PM, Khaddaj-Mallat, C, Alessandrini, B, and Ferrant, P (2010). "SPH simulation of green water and ship flooding scenarios," *Journal of Hydrodynamics*, 22(5), 231-236.
- Luo, M, Khayyer, A, Lin, P (2021). "Particle methods in ocean and coastal engineering," *Applied Ocean Research*, 114, 102734.
- Nielsen, KB, and Mayer, S (2004). "Numerical prediction of green water incidents," *Ocean Engineering*, 31(3-4), 363-399.
- Rosetti, GF, Pinto, ML, de Mello, PC, Sampaio, CMP, Simos, AN, and Silva, DFC (2019). "CFD and experimental assessment of green water events on an FPSO hull section in beam waves," *Marine Structures*, 65, 154-180.
- Shibata, K, and Koshizuka, S (2007). "Numerical analysis of shipping water impact on a deck using a particle method," *Ocean Engineering*, 34(3-4), 585-593.
- Shibata, K, Koshizuka, S, Sakai, M, and Tanizawa, K (2012). "Lagrangian simulations of ship-wave interactions in rough seas," *Ocean Engineering*, 42, 13-25.
- Silva, DFC, Esperanca, PTT, and Coutinho, ALGA (2017). "Green water loads on FPSOs exposed to beam and quartering seas, Part II: CFD simulations," *Ocean Engineering*, 140, 434-452.
- Tanaka, M, and Masunaga, T (2010). "Stabilization and smoothing of pressure in MPS method by Quasi-Compressibility," *Journal of Computational Physics*, 229(11), 4279-4290.
- Tang, Z, Wan, D, Chen, G, and Xiao, Q (2016). "Numerical simulation of 3D violent free-surface flows by multi-resolution MPS method," *Journal of Ocean Engineering and Marine Energy*, 2(3), 355-364.
- Tang, Z, Zhang, Y, and Wan, D (2016). "Multi-Resolution MPS Method for Free Surface Flows," *International Journal of Computational Methods*, 13(4), 1641018.
- Wen, X, Zhao, W, and Wan, D (2021). "An improved moving particle semi-implicit method for interfacial flows," *Applied Ocean Research*, 117, 102963.
- Ye, Z, and Zhao, X (2017). "Investigation of water-water interface in dam break flow with a wet bed," *Journal of Hydrology*, 548, 104-120.
- Zhang, G, Chen, X, and Wan, D (2019). "MPS-FEM Coupled Method for Study of Wave-Structure Interaction," *Journal of Marine Science and Application*, 18(4), 387-399.
- Zhang, S, Yue, DK-P, and Tanizawa, K (1996). "Simulation of plunging wave impact on a vertical wall," *Journal of Fluid Mechanics*, 327, 221-254.
- Zhang, Y, Tang, Z, and Wan, D (2016). "Simulation of solitary wave interacting with flat plate by MPS method," *Chinese Journal of Hydrodynamics*, 31(4), 821-831.
- Zhang, Y, Wan, D, Hino, T (2014). "Application of MPS method in liquid sloshing," *Ocean Engineering*, 32(4), 24-32.